David Tomás Sánchez Martínez
Lourdes García Rodríguez
(coordinadores)

Proceedings of the 7th International Seminar on ORC Power Systems

Editorial Universidad de Sevilla

Proceedings of the 7th International Seminar on

ORC

Power Systems

David Tomás Sánchez Martínez
Lourdes García Rodríguez
(coordinadores)

Proceedings of the 7th International Seminar on

ORC Power Systems

(ORC2023)

4th to 6th
SEPTEMBER
SEVILLE 2023

EDITORIAL UNIVERSIDAD DE SEVILLA

Sevilla, 2024

Colección Actas
Núm.: 91

Review chairs of the 7th International Seminar on ORC Power Systems

Prof. Christoph Wieland (University of Duisburg-Essen) - *Review Chair*
Prof. Sotirios Karellas (National Technical University of Athens) - *Review Co-Chair*
Prof. Teemu Turunen-Saaresti (LUT University) - *Review Co-Chair*
Dr. Diego-César Alarcón-Padilla (Plataforma Solar de Almería - CIEMAT) - *Review Co-Chair*
Dr. Francesco Crespi (Universidad de Sevilla) - *Review Co-Chair*

c/ Porvenir, 27 - 41013 Sevilla.
Tlfs.: 954 487 447; 954 487 451; Fax: 954 487 443
Correo electrónico: info-eus@us.es
Web: https://editorial.us.es

ISBN 978-84-472-2745-7
DOI: https://dx.doi.org/10.12795/9788447227457

Diseño de cubierta y maquetación: los autores

INDEX OF CONTRIBUTIONS

DOI: https://dx.doi.org/10.12795/9788447227457_37

INVESTIGATING R1234ZE AND R1234YF AS REPLACEMENTS TO R134A IN WASTE HEAT RECOVERY ORC APPLICATIONS

James Bull*, James Buick, Jovana Radulovic

[1] *University Of Portsmouth, Anglesea Rd, Portsmouth PO1 3DJ*

*Corresponding Author: james.bull@port.ac.uk

ABSTRACT

The ever-growing energy demand across the globe puts significant pressure on the power generation sector to find renewable and sustainable alternatives to fossil fuels. Organic Rankine Cycle (ORC) technology can be applied to low-medium temperature heat sources to generate useful work. In this paper, an ORC cycle, powered by a medium temperature exhaust gas at 423.15 K, is modelled. Working fluids R1234ze and R1234yf were compared as replacements to R134a and considered across a variety of operating conditions comparing both the energetic and exergetic performance. Sizing of heat exchangers (evaporator and condenser) has also been undertaken. Following a comprehensive evaluation, R1234ze is recommended as a viable replacement to R134a, specifically regarding the pump and turbine performance.

1 INTRODUCTION

Increasing global energy demand has put significant strain on the energy sector to find alternative sources to the finite fossil fuels in order to reduce global warming and ozone depletion. Researchers have concentrated on two primary strategies to tackle these challenges: enhancing the utilization of renewable and sustainable energy sources and optimizing the efficiency of energy systems to maximize energy utilization from a source.

The five main renewable energy sources can be categorized into the following; hydropower, biomass, solar, wind and geothermal. Hydropower has the greatest benefit within energy storage systems due to large capacity and low cost, however in many cases it requires an initial resource investment to create the storage in the first place (Zhao et al., 2022). Biomass energy plays a significant role in eliminating fossil fuel use, specifically in countries with an abundance of bioresources (Vallios et al., 2009). Solar, wind and geothermal energy are all important renewable energy sources with high potential for energy generation. Li et al. (2015) compared the use of geothermal power plants against the solar and wind generation systems and identified significant advantages for the former. Specifically, geothermal power generation demonstrated greater stability in power output in higher capacity with a lower ecological effect. Bett and Thornton (2016) further supported this when analyzing the impact climate has on the wind and solar power across Britain. The results show that the seasonal variability in potential power generated for solar and wind is up to 70% and 30%, respectively, across the year.

An alternative to renewable and sustainable energy sources is that of waste heat recovery (WHR). Waste heat recovery allows the utilization of otherwise wasted heat energy from industrial processes, power generation, or other sources. By capturing and reusing this heat, energy efficiency is significantly improved. This reduces the overall energy consumption and the reliance on primary energy sources, leading to lower greenhouse gas emissions and a more sustainable use of resources (Zhang & Akiyama, 2009). Waste heat recovery possesses several advantages compared to the renewable energy sources described above. Since WHR is an integrated application to existing processes, it does not require land development or resource extraction. Additionally, WHR also exhibits a high potential utilization factor compared to solar or wind energies (Jung et al., 2014). Various technologies can be employed to harness WHR, such as the organic Rankine cycle (ORC) (Galanis et al., 2009). The Organic Rankine Cycle (ORC) is one of the most versatile power cycle technologies implemented in a variety of low-medium temperature scenarios . While similar to the conventional Rankine cycle, the ORC utilizes refrigerants or organic substances as working fluids instead of water. This allows for the recovery of energy from low-temperature waste heat sources, facilitated by the lower boiling points of organic working fluids compared to water (Nguyen et al., 2010).

Arguably, the most important aspect of designing an ORC system is the working fluid selection. Over the years many researchers have investigated the working fluid selection against a range of operational conditions and system components (Bao & Zhao, 2013; Campos Rodríguez et al., 2013; Özcan & Ekici, 2021; Zeyghami, 2015). Specifically, one of the most used working fluids in a variety of low-medium grade ORC applications is R134a (Lai et al., 2011; Quoilin et al., 2013; Saleh et al., 2007; Shengjun et al., 2011). Environmentally speaking, although R134a has an Ozone Depletion Potential (ODP) of 0, it is a hydrofluorocarbon (HFC) with a global warming potential GWP of 1430 (Lemmon et al., 2018). This is of significant importance based on the harmful impact high GWPs has on the environment and the subsequent regulations implemented to phase out such working fluids (Schulz & Kourkoulas, 2014). Two working fluids often used to replace R134a are R1234ze and R1234yf, both of which having an ODP of 0 and GWP of 6 and 4, respectively (Lemmon et al., 2018). Yamada, Mohamad, and Kien (2012) highlighted that comparing R134a to a selection of working fluids in a basic ORC, both R1234ze and R1234yf displayed similar performance. Le et al. (2014) optimized a basic and regenerative supercritical ORC and identified R1234ze as the best working fluid for net power against R134a. Moles et al. (2017) directly compared R1234yf and R1234ze against R134a within a basic and regenerative cycle. The main findings presented indicate both fluids offer similar performance to R134a at lower evaporating temperatures. However, as the evaporating temperature increases R1234yf requires a higher pump power and produces a lower net cycle efficiency, whereas, R1234ze requires lower pump power and produces higher pump efficiency.

From the literature above it is clear there is a need not only to investigate ORC systems for waste heat recovery, but also to aide the expanse of research dedicated to identifying suitable replacements to R134a. Therefore, this paper aims to add to the existing working fluid evaluations of R134a replacements by comparing the performance against R1234ze and R1234yf. The working fluids are evaluated through modelling an ORC system heated by exhaust gas at 423.15 K. The comparison will include a heat exchanger sizing for the evaporator and condenser. An energetic and exergetic analysis of the ORC system will be considered to establish both the thermodynamic performance and assess the areas of energy waste between the working fluids.

2 METHODOLOGY

2.1 Organic Rankine Cycle

The ORC configuration and T-S diagram for the system setup is shown in Figure 1. The assumptions made for the cycle include no system heat losses and no pressure drop within the pipework. In order to complete the energetic and exergetic analysis, REFPROP was used to determine the required properties of the working fluids considered (Lemmon et al., 2018). The heating fluid was set as exhaust air and the cooling fluid was set as water. Table 1 demonstrates the assumed variables for the energetic and exergetic analysis.

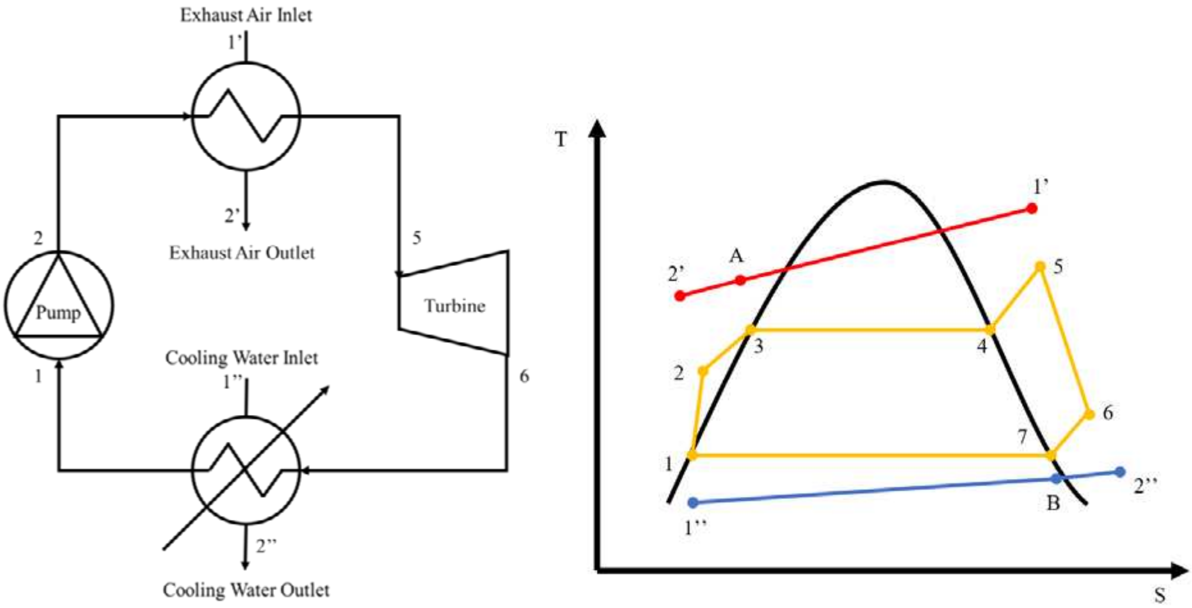

Figure 1: Organic Rankine Cycle configuration and T-S diagram

Table 1: Assumed parameters for the energetic and exergetic analysis

Variable	Value	Variable	Value
Ambient temperature	298.15 K	Condenser Pinch Point	10 K
Heating Fluid inlet Temperature	423.15 K	Pump inlet Temperature	293.15 K
Cooling Fluid inlet Temperature	278.15 K	η_{Pump}	80%
Approach Temperature	20 K	$\eta_{Turbine}$	70%
Evaporator Pinch Point	20 K		

236

The maximum temperature of the ORC was determined from the heating fluid inlet temperature minus the approach temperature. The maximum pressure of each working fluid was set as the saturated liquid pressure at 363.15 K. The energetic and exergetic analysis was completed using equations (1)-(10) (Cengel et al., 2011; Dincer & Rosen, 2012).

$$\eta_{Pump} = \frac{h_2 - h_1}{h_{2is} - h_1} \tag{1}$$

$$\eta_{Turbine} = \frac{h_5 - h_6}{h_5 - h_{6is}} \tag{2}$$

$$W_{Net} = W_{Turbine} - W_{Pump} = (h_5 - h_6) - (h_2 - h_1) \tag{3}$$

$$Q_{in} = h_5 - h_2 \tag{4}$$

$$\eta_{Cycle} = \frac{W_{Net}}{Q_{in}} \tag{5}$$

The exergy efficiency was evaluated using equation (6).

$$\eta_{ex} = \frac{W_{Net}}{Q_{in}\left(1 - \frac{T_0}{T_5}\right)} \tag{6}$$

And the exergy destruction for each component of the cycle was calculated using equations (7)-(10).

$$Ex_{D,E} = \dot{m}_{wf}\big((h_5 - T_0 s_5) - (h_2 - T_0 s_2)\big) + \dot{m}_{wf}(h_5 - h_2)\left(1 - \frac{T_0}{T_5}\right) \tag{7}$$

$$Ex_{D,T} = \dot{m}_{wf}\big((h_5 - T_0 s_5) - (h_6 - T_0 s_6)\big) + \dot{m}_{wf}(h_5 - h_6) \tag{8}$$

$$Ex_{D,C} = \dot{m}_{wf}\big((h_6 - T_0 s_6) - (h_1 - T_0 s_1)\big) \tag{9}$$

$$Ex_{D,P} = \dot{m}_{wf}\big((h_2 - T_0 s_2) - (h_1 - T_0 s_1)\big) + \dot{m}_{wf}(h_2 - h_1) \tag{10}$$

2.2 Heat Exchanger

There are three primary types of heat exchangers frequently used: fin and tube, plate, and shell and tube configurations. To maintain consistency in modeling the evaporator and condenser for all fluids, a shell and tube configuration is chosen. This configuration is preferred due to its versatility in accommodating various temperature ranges and fluid states between the hot and cold sides. The configuration for the shell and tube heat exchangers is that of TEMA type E, shown in Figure 2.

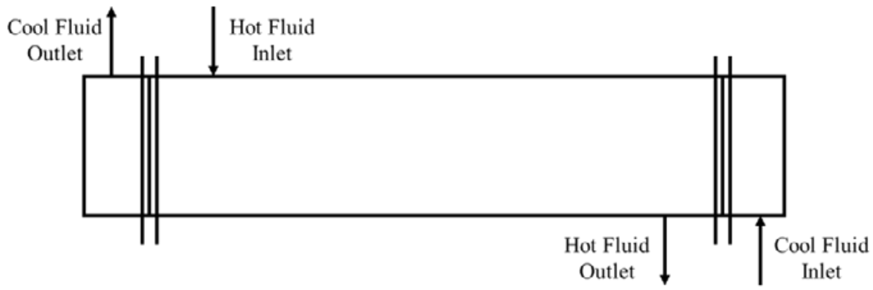

Figure 2: Shell and Tube Heat Exchanger Configuration TEMA Type E

The methodology used is off the work done by Bull et al. (2020) using the shell and tube heat exchanger design methodology from (Kakac et al., 2020; Kern, 1983). To account for the phase change of the working fluid, the evaporator calculations were split into three sections: pre-heater, phase change and super heater. The condenser calculations were split into two sections: phase change and super heater. To split the sections, the appropriate heating and cooling fluid temperatures were calculated from the corresponding working fluid phase change temperatures with the general energy balance equation shown in equation (11). 237

$$\dot{m}_{wf}(h_{out} - h_{in}) = \dot{m}_{hf/cf} C_{p,hf/cf}(T_{out} - T_{in}) \tag{11}$$

Where the $\dot{m}_{hf/cf}$ and $C_{p,hf/cf}$ is the mass flow rate and the specific heat capacity of the heating/cooling fluid respectively. The mass flow rate for each working fluid was fixed at the required mass flow rate for the ORC to output 10 kW of power. In order to size the heat exchanger, the shell and tubes diameters were set as 0.06 m and 0.01 m, respectively, and 1 shell pass with 2 tubes. In addition, the heat exchanger was modelling with negligible tube thickness and no fouling or baffles. For each section, average values for density, viscosity, specific heat capacity and thermal conductivity were calculated through REFPROP.

2.2.1 Pre-heat and Super heat

To calculate the heat transfer area required the log mean temperature difference was determined by equation (12).

$$\Delta T_{LMCF} = \frac{\Delta T_1 - \Delta T_2}{\ln\left(\frac{\Delta T_1}{\Delta T_2}\right)} \tag{12}$$

With correction factor (F) incorporated for the pre-heater and super-heater sections defined by equation (13) and subsequent corrected LMTD given by equation (14):

$$F = \frac{\sqrt{R^2+1}}{(R-1)} \frac{\ln\left(\frac{1-P}{1-PR}\right)}{\ln\left(\frac{\frac{2}{P}-1-R+\sqrt{R^2+1}}{\frac{2}{P}-1-R-\sqrt{R^2+1}}\right)} \tag{13}$$

$$\Delta T_{LM} = \Delta T_{LMCF} F \tag{14}$$

The overall heat transfer coefficient was determined by equation (15):

$$U = \frac{1}{\frac{1}{h_{wf}} + \frac{1}{h_{hf/cf}}} \tag{15}$$

Where the heat transfer coefficient for the working fluid side and the thermal fluid side are given by equation (16):

$$h = \frac{Nu\, k}{D} \tag{16}$$

The values for the Nusselt number were calculated using the Dittus-Boelter correlation shown in equation (17):

$$Nu = 0.023 Re^{0.8} Pr^{n} \tag{17}$$

The heating exponent, n, is 0.4 and 0.3 for the cold fluid and hot fluid respectively. The required heat transfer area is calculated using equation (18):

$$A = \frac{Q_{ht}}{U \Delta T_{LM}} \tag{18}$$

Where the heat transferred for each section is calculated using equation (19):

$$Q_{ht} = \dot{m}_{wf}(h_{out} - h_{in}) \tag{19}$$

2.2.2 Phase Change

The Shah correlation (Shah, 1979) for two-phase flow was additionally incorporated for the heat transfer coefficient in the phase change section for the evaporator and condenser using equation (20):

$$h_{lv} = h_l \left[(1-x)^{0.8} + \frac{3.8x^{0.76}(1-x)^{0.04}}{p_r^{0.38}}\right] \tag{20}$$

Where the mixture, x, was averaged to 0.5 and the reduced pressure was calculated with the critical fluid pressure using equation (21):

$$p_r = \frac{p_{crit}}{p_2} \tag{21}$$

2.2.2 Pressure Drop

The Pressure drop for the heat exchangers was calculated using equations (22) and (23):

$$\Delta p_t = \frac{2 f_t L \rho u_t^2}{D_t} \tag{22}$$

$$\Delta p_s = \frac{f_s G_s^2 D_s}{2 \rho D_e} \tag{23}$$

Where the respective friction factors are given by equations (24) and (25):

$$f_t = (1.58 \ln(Re_t) - 3.28)^{-2} \tag{24}$$

$$f_s = e^{(0.576-0.19\ln(Re_s))} \quad (25)$$

3 RESULTS

The following results include the respective adjustments to the evaporation and condensation pressure for each fluid based on the pressure drop calculated. The energetic performance characteristics is compared for each fluid and shown within Table 2. A percentage comparison of the energetic performance characteristics is shown in Table 3.

Table 2: Comparison of energetic analysis results

Fluid Name	Mass Flow (kg/s)	Net Power (kW)	Pump Power (kW)	Turbine Power (kW)	Rate of Heat In (kW)	Efficiency (%)	Back Work Ratio
R134a	0.271	8.622	0.654	9.276	71.10	12.127	0.071
R1234ze	0.285	8.503	0.548	9.051	73.49	11.571	0.061
R1234yf	0.320	8.530	0.794	9.324	76.05	11.217	0.085

Table 3: Percentage comparison of energetic analysis results against R134a

Fluid Name	Mass Flow (%)	Net Power (kW)	Pump Power (%)	Turbine Power (%)	Heat In (%)	Back Work Ratio (%)
R1234ze	5.087	-1.381	-16.229	-2.428	3.360	-14.144
R1234yf	18.155	-1.071	21.345	0.510	6.960	20.729

Based on the cycle parameters set within the methodology, R134a required the lowest mass flow rate and achieved the highest cycle efficiency of 0.271 kg/s and 12.127 %, respectively. Interestingly, R1234ze required the lowest pump power of 0.548 kW, and subsequently, generated the lowest turbine output power of 9.051 kW. However, R1234ze required 16.229 % less pump power compared to R134a in order to generate only 2.428 % less turbine power and achieve 1.381 % less net power. This result is further reflected by the back work ratio as R1234ze has the lowest with a value of 0.061, a 14.144 % drop from that of R134a. On the other hand, R1234yf displayed contrasting results, requiring the highest pump power, heat input, turbine power output, and subsequently displaying the highest back work ratio with the lowest cycle efficiency. Based on the energetic analysis conducted, despite favorable performance shown from R134a, R1234ze could be used as a suitable replacement in an ORC of this nature. 239

Table 4: A comparisons of exergetic analysis results

Fluid Name	Evaporator (kW)	Turbine (kW)	Condenser (kW)	Pump (kW)	Exergy Efficiency
R134a	29.408	21.599	61.545	1.155	46.583
R1234ze	30.290	20.989	64.616	0.967	44.430
R1234yf	31.340	21.616	67.370	1.405	43.069

Table 5: A percentage comparison of exergetic analysis results against R134a

Fluid Name	Evaporator (%)	Turbine (%)	Condenser (%)	Pump (%)
R1234ze	2.999	-2.823	4.989	-16.262
R1234yf	6.570	0.081	9.463	21.639

Table 4 demonstrates a comparison of the exergetic analysis results and Table 5 highlights the percentage comparison against R134a. Overall, R134a displayed the lowest exergy destruction for the evaporation and condenser components of the ORC. Additionally, R134a had the highest exergy efficiency of 46.583 % indicating increased reversibility of the system. Taking into consideration the exergy destruction reported at each component, R1234ze showed lower exergy destruction compared to R134a in both the turbine and pump by 2.823 % and 16.262 %, respectively. However, R1234yf not only demonstrated the lowest exergy efficiency of 43.069 %, it also had the highest exergy destruction across all components of the cycle presented. Similar to the energetic analysis, the exergetic analysis indicates that R1234ze proves to be a favorable replacement to R134a, especially when considering the fluid performance through the pump and turbine sections of the ORC.

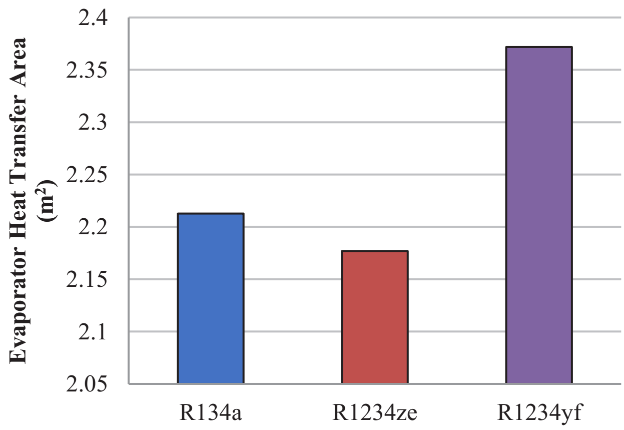

Figure 3: Evaporator heat transfer area required

Figure 3 demonstrates the heat transfer area required through the evaporator section of the ORC. The area required for R134a, R1234ze and R1234yf was calculated as 2.212 m^2, 2.177 m^2 and 2.371 m^2, respectively. Although R134a displayed the lowest mass flow rate and lowest heat in, shown in Table 2, R1234ze demonstrated the lowest area required for the heat exchanger. In contrast, R1234yf demonstrated the highest heat transfer area required. A similar correlation can be noted for the condenser heat exchanger sizing. Figure 4 presents a comparison of the heat transfer area required for the condenser section of the ORC. Overall, R1234yf has the highest area required of 31.768 m^2. Whereas R1234ze displays the lowest area of 29.347 m^2. 240

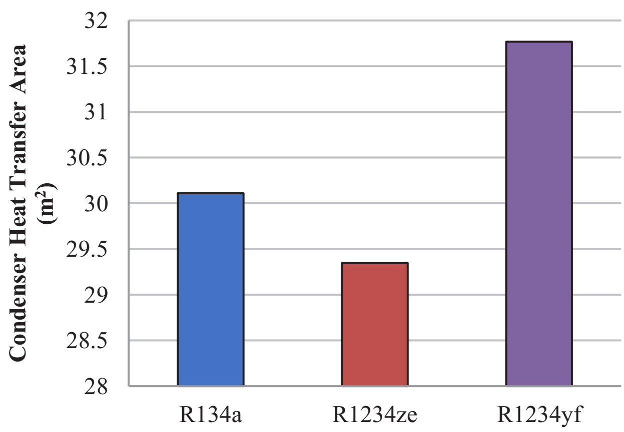

Figure 4: Condenser heat transfer area required

4 CONCLUSIONS

The results present in this study indicate the following conclusions:

- Based on the energetic analysis, although R134a displayed the best overall performance, R1234ze could be used as a suitable alternative.
- During the exergetic analysis, R1234ze proved to be a suitable replacement especially through the pump and turbine sections of the ORC.
- In both the condenser and evaporator heat exchanger sizing, R1234ze demonstrated the lowest area required.
- In all aspects evaluated within this paper, R1234yf would not be recommended as a suitable replacement to R134a.

NOMENCLATURE

T	Temperature
p	Pressure
η	Efficiency
W	Work done
h	Enthalpy
Q	Heat
Ex	Exergy
s	Entropy
$\dot{m}$	Mass Flow Rate
C_p	Specific Heat Capacity
U	Heat Transfe r Coefficient
D	Diameter
Nu	Nusselt Number
Re	Reynolds Number
Pr	Prandtl Number
A	Heat Transfer Area
ρ	Density
G	Mass Flux
f	Friction Factor
u	Velocity
L	Heat Exchanger Length
Subscript	
1,2,3,4,5,6,7	Position in ORC
is	isentropic
ex	Exergy
D	Destruction
P	Pump
E	Evaporator
T	Turbine
C	Condenser
0	Ambient Conditions
wf	Working Fluid
hf	Heating Fluid
cf	Cooling Fluid
in	Generalized Reference Inlet
out	Generalized Reference Outlet
LM	Log Mean
ht	Heat Transferred
lv	Liquid-Vapor Phase
crit	Critical Point
r	Ratio

s	Shell
t	Tube

REFERENCES

Bao, J., & Zhao, L. (2013). A review of working fluid and expander selections for organic Rankine cycle. *Renewable and Sustainable Energy Reviews*, *24*, 325–342.

Bett, P. E., & Thornton, H. E. (2016). The climatological relationships between wind and solar energy supply in Britain. *Renewable Energy*, *87*, 96–110. https://doi.org/10.1016/j.renene.2015.10.006

Bull, J., Buick, J. M., & Radulovic, J. (2020). Heat exchanger sizing for organic rankine cycle. *Energies*, *13*(14), 1–10. https://doi.org/10.3390/en13143615

Campos Rodríguez, C. E., Escobar Palacio, J. C., Venturini, O. J., Silva Lora, E. E., Cobas, V. M., Marques Dos Santos, D., Lofrano Dotto, F. R., & Gialluca, V. (2013). Exergetic and economic comparison of ORC and Kalina cycle for low temperature enhanced geothermal system in Brazil. *Applied Thermal Engineering*, *52*(1), 109–119. https://doi.org/10.1016/j.applthermaleng.2012.11.012

Cengel, Y. A., Boles, M. A., & Kano\uglu, M. (2011). *Thermodynamics: an engineering approach* (Vol. 5). McGraw-hill New York.

Dincer, I., & Rosen, M. A. (2012). *Exergy: energy, environment and sustainable development*. Newnes.

Galanis, N., Cayer, E., Roy, P., Denis, E. S., & Désilets, M. (2009). Electricity generation from low temperature sources. *Journal of Applied Fluid Mechanics*, *2*(2), 55–67. https://doi.org/10.36884/jafm.2.02.11870

Jung, H. C., Krumdieck, S., & Vranjes, T. (2014). Feasibility assessment of refinery waste heat-to-power conversion using an organic Rankine cycle. *Energy Conversion and Management*, *77*, 396–407. https://doi.org/https://doi.org/10.1016/j.enconman.2013.09.057

Kakac, S., Liu, H., & Pramuanjaroenkij, A. (2020). *Heat exchangers: selection, rating, and thermal design*. CRC press.

Kern, D. (1983). *Process Heat Transfer*. Tosho Printing Co., LTD.

Lai, N. A., Wendland, M., & Fischer, J. (2011). Working fluids for high-temperature organic Rankine cycles. *Energy*, *36*(1), 199–211. https://doi.org/10.1016/j.energy.2010.10.051

Le, V. L., Feidt, M., Kheiri, A., & Pelloux-Prayer, S. (2014). Performance optimization of low-temperature power generation by supercritical ORCs (organic Rankine cycles) using low GWP (global warming potential) working fluids. *Energy*, *67*, 513–526. https://doi.org/10.1016/j.energy.2013.12.027

Lemmon, E. W., Bell, and I. H., Huber, M. L., & McLinden, M. O. (2018). *NIST Standard Reference Database 23: Reference Fluid Thermodynamic and Transport Properties-REFPROP, Version 10.0, National Institute of Standards and Technology*. https://www.nist.gov/srd/refprop

Li, K., Bian, H., Liu, C., Zhang, D., & Yang, Y. (2015). Comparison of geothermal with solar and wind power generation systems. *Renewable and Sustainable Energy Reviews*, *42*, 1464–1474.

Moles, F., Navarro-Esbrí, J., Peris, B., Mota-Babiloni, A., & Mateu-Royo, C. (2017). R1234yf and R1234ze as alternatives to R134a in Organic Rankine Cycles for low temperature heat sources. *Energy Procedia*, *142*, 1192–1198.

Nguyen, T. Q., Slawnwhite, J. D., & Boulama, K. G. (2010). Power generation from residual industrial heat. *Energy Conversion and Management*, *51*(11), 2220–2229.

Özcan, Z., & Ekici, Ö. (2021). A novel working fluid selection and waste heat recovery by an exergoeconomic approach for a geothermally sourced ORC system. *Geothermics*, *95*(November 2020). https://doi.org/10.1016/j.geothermics.2021.102151

Quoilin, S., Van Den Broek, M., Declaye, S., Dewallef, P., & Lemort, V. (2013). Techno-economic survey of Organic Rankine Cycle (ORC) systems. *Renewable and Sustainable Energy Reviews*, *22*, 168–186. https://doi.org/https://doi.org/10.1016/j.rser.2013.01.028

Saleh, B., Koglbauer, G., Wendland, M., & Fischer, J. (2007). Working fluids for low-temperature organic Rankine cycles. *Energy*, *32*(7), 1210–1221. https://doi.org/10.1016/j.energy.2006.07.001

Schulz, M., & Kourkoulas, D. (2014). Regulation (EU) No 517/2014 of The European Parliament and of the council of 16 April 2014 on fluorinated greenhouse gases and repealing Regulation (EC)

No 842/2006. *Off. J. Eur. Union*, *2014*(517), L150.
Shah, M. M. (1979). A general correlation for heat transfer during film condensation inside pipes. *International Journal of Heat and Mass Transfer*, *22*(4), 547–556.
Shengjun, Z., Huaixin, W., & Tao, G. (2011). Performance comparison and parametric optimization of subcritical Organic Rankine Cycle (ORC) and transcritical power cycle system for low-temperature geothermal power generation. *Applied Energy*, *88*(8), 2740–2754.
Vallios, I., Tsoutsos, T., & Papadakis, G. (2009). Design of biomass district heating systems. *Biomass and Bioenergy*, *33*(4), 659–678. https://doi.org/10.1016/j.biombioe.2008.10.009
Yamada, N., Mohamad, N., & Kien, T. (2012). Study on thermal efficiency of low- to medium-temperature organic Rankine cycles using HFO−1234yf. *Renewable Energy*, *41*, 368–375.
Zeyghami, M. (2015). Performance analysis and binary working fluid selection of combined flash-binary geothermal cycle. *Energy*, *88*, 765–774. https://doi.org/10.1016/j.energy.2015.05.092
Zhang, L., & Akiyama, T. (2009). How to recuperate industrial waste heat beyond time and space. *International Journal of Exergy*, *6*(2), 214–227.
Zhao, J. F., Oh, U. J., Park, J. C., Park, E. S., Im, H. Bin, Lee, K. Y., & Choi, J. S. (2022). A Review of World-wide Advanced Pumped Storage Hydropower Technologies. *IFAC-PapersOnLine*, *55*(9), 170–174. https://doi.org/10.1016/j.ifacol.2022.07.030

This book contains the compilation of works contributed to the *7th International Seminar on Organic Rankine Cycle Power Systems* (ORC 2023), held in Seville between the 4th and 6th of September 2023. The event was hosted by Universidad de Sevilla on behalf of the Knowledge Centre on Organic Rankine Cycle Technology (KCORC), incorporated in The Netherlands.

The ORC conference, organized biennially, stems as the only conference that is specific to ORC technology, therefore gathering a diverse community whose affiliation spans across all the interested stakeholders, not only in this particular technology but also and in a broader context, in the energy transition. Original equipment manufacturers, professional associations, end-users, investors, policy makers, academics, scientists feel at home at ORC 2023.

The almost 100 proceedings in this book cover a wide variety of topics, from fundamentals to system integration through component design, accounting for thermodynamic performance as well as component design. In addition to this, and as a new track in 2023, works on heat pump technology were also accepted in order to raise awareness of the strong ties between both technologies, specifically in energy storage applications.

This book provides an excellent overview of the current maturity of power systems based on Organic Rankine Cycle technology for applications as diverse as geothermal and waste heat recovery in industry or downstream of other prime movers (e.g., marine applications). It is also an excellent source of information to understand the current challenges faced by the technology, stemming from a very competitive market and increasingly stringent environmental regulations.

The organizers of ORC 2023 hope that the reader finds this work as exciting as the attendees to the conference and, maybe, make the decision to join the 8th edition to the conference in 2025.

KCORC
KNOWLEDGE CENTER
ORGANIC RANKINE CYCLE

eUS EDITORIAL
UNIVERSIDAD DE SEVILLA